

1 FIND: A Synthetic weather generator to control  
2 drought Frequency, Intensity, and Duration

3 Marta Zaniolo<sup>a</sup>, Sarah Fletcher<sup>a,b,c</sup>, Meagan Mauter<sup>a,b,c</sup>

<sup>a</sup>*Civil and Environmental Engineering Department, 473 Via  
Ortega, Stanford, 94305, California, USA*

<sup>b</sup>*Woods Institute for the Environment, 473 Via  
Ortega, Stanford, 94305, California, USA*

<sup>c</sup>*Authors equally contributed to the work.*

---

4 **Abstract**

5 Water systems worldwide are experiencing climate change-induced shifts in  
6 drought properties like frequency, intensity, and duration, affecting water  
7 security and reliability. To develop and test effective drought preparedness  
8 plans, researchers often use synthetic weather generators to create hydrolog-  
9 ical scenarios that explore drought variability beyond historical records. Ex-  
10 isting weather generators typically allow users to adjust streamflow statistics  
11 like percentiles or temporal correlation but do not directly control drought  
12 properties of frequency, intensity, and duration. To fill this gap, we pro-  
13 pose FIND (Frequency, INTensity, and Duration) synthetic weather gener-  
14 ator. FIND incorporates a standardized drought index to directly and in-  
15 dependently control drought frequency, intensity, and duration in generated  
16 streamflow time series while preserving observed hydrological variability. Use  
17 cases for FIND include i) water systems analysis applications that seek to  
18 train and test drought strategies under historical and plausible future drought  
19 conditions, and ii) bottom-up vulnerability studies relating system vulner-  
20 ability outcomes to specific changes in drought properties of frequency, in-  
21 tensity, and duration. We demonstrate FIND’s versatility through three  
22 experiments: replicating historically observed drought properties, generating  
23 streamflow scenarios for multiple sites preserving correlation between their  
24 drought conditions, and generating a set of scenarios with direct and inde-  
25 pendent changes in drought properties. FIND source code is openly available  
26 for applications beyond the scope of this paper.

27 *Keywords:* synthetic weather generator, drought properties, bottom-up

## 29 1. Introduction

30 Changes in drought frequency, intensity, and duration are expected to  
31 challenge water systems worldwide. However, shifts in these drought prop-  
32 erties are expected to occur at different rates and magnitudes (Naumann  
33 et al., 2018) and produce different impacts. First, future changes in drought  
34 frequency, intensity, and duration may be fueled by different climate mecha-  
35 nisms. For example, changes in atmospheric circulation patterns and cyclic  
36 climate phenomena such as El Niño Southern Oscillation (ENSO) can lead to  
37 longer and more intense droughts (Singh et al., 2022). Land use change and  
38 deforestation can contribute to faster and more intense droughts (de Jager  
39 et al., 2022), while local evapotranspiration increase may drive more frequent  
40 and intense droughts (Aadhar and Mishra, 2020). Second, changes in certain  
41 drought properties may yield disproportionate effects on a water system. For  
42 instance, some systems may be more susceptible to rising drought intensity  
43 compared to longer drought duration (Zaniolo et al., 2023).

44 In water system literature, climate adaptation studies often rely on sam-  
45 pling future climate scenarios to test system resilience to climate change.  
46 Two approaches are commonly recognized. The top-down approach simu-  
47 lates the system under an ensemble of future climate scenarios derived from  
48 global circulation models and ran under different greenhouse gas emission  
49 scenarios. These ensembles are a lower bound on the uncertainty in climate  
50 impacts (Stainforth et al., 2007), and underestimating uncertainty can make  
51 planning decisions vulnerable to failure (Bryant and Lempert, 2010; Brown  
52 et al., 2012). In addition, these ensembles focus on capturing long-term  
53 climate change trends, but they are known to underestimate the impact of  
54 short-term extremes like droughts (Johnson et al., 2011; Rocheta et al., 2014;  
55 Tallaksen and Stahl, 2014). Bottom-up, vulnerability-based approaches of-  
56 fer an alternative for water system adaptation in the near term (Borgomeo  
57 et al., 2015b). Instead of aiming for precise predictions of future climate,  
58 these approaches sample relevant hydroclimatic variables within predefined  
59 plausible ranges to assess the system’s response to changes (Herman et al.,  
60 2015). Bottom-up approaches can identify changes in specific variables or  
61 combinations of variables that drive water system vulnerability, including  
62 changes in drought properties.

63 Bottom-up methods rely on synthetic weather generators for the genera-  
64 tion of a large sampling of plausible hydroclimatic scenarios. These genera-  
65 tors aim to preserve certain characteristics of the local climate, such as annual  
66 variability, while modifying specific variables of interest for the bottom-up  
67 analysis. Some studies focus on changes to relevant hydroclimatic statis-  
68 tics, for example by applying a change factor to simulate shifts in the mean  
69 or lower percentiles of precipitation, temperature, or streamflow (Hall and  
70 Borgomeo, 2013; Yang et al., 2016; Ray et al., 2018; Giuliani et al., 2022).  
71 Other methods alter the temporal dependence structure of hydroclimatic  
72 time series, for instance by modifying the seasonality or the persistence of  
73 wet and dry conditions. Various techniques are used for this purpose, includ-  
74 ing Markov chain models (Breinl et al., 2015; Ullrich et al., 2021), spectral  
75 analysis and wavelet transforms (Steinschneider and Brown, 2013; Quinn  
76 et al., 2018; Fletcher et al., 2023), and copula methods (Borgomeo et al.,  
77 2015b; Nazemi et al., 2020). Lastly, Borgomeo et al. (2015a) proposes a ver-  
78 satile tool that lets the user choose the objective function of the streamflow  
79 generator to optimize the streamflow properties of interest.

80 Current bottom-up approaches have limitations when modeling changes  
81 in drought properties. The manipulation of specific hydroclimatic statistics  
82 can impact the drought properties of the generated scenarios, but only in-  
83 directly. For instance, shifting the mean of a streamflow scenario can lead  
84 to more intense and longer droughts, and altering the streamflow tempo-  
85 ral structure can result in longer or more frequent droughts compared to  
86 historical observations. However, the relationship between the change in a  
87 hydrological statistic and the change in drought property is not linear and not  
88 quantified. Moreover, changes in a hydrological statistic may typically affect  
89 more than one drought property. Therefore, the precise quantification, inde-  
90 pendent manipulation, and systematic evaluation of the effects of changes in  
91 drought properties on a system remain challenging. As a result, it becomes  
92 difficult to parse out the impacts of comparable changes in drought frequency,  
93 intensity, and duration on system vulnerability directly and independently.

94 Drought indices offer a way to quantify the magnitude and change of  
95 drought properties. These indices are functions of hydroclimatological vari-  
96 ables (e.g., precipitation, temperature, streamflow) and they can provide a  
97 standardized measure of drought based on statistical analysis and compar-  
98 isons with historical data. One notable streamflow generator that incorpo-  
99 rates a drought index is the approach presented in Herman et al. (2016), that  
100 uses the Standardized Streamflow Index (SSI, Vicente-Serrano and López-

101 Moreno (2005)) to quantify drought frequency and severity. However, this  
102 generator does not allow for independent manipulation of these two at-  
103 tributes.

104 We propose FIND (Frequency, INtensity, and Duration), a synthetic  
105 drought generator designed to generate streamflow or precipitation scenar-  
106 ios with specific drought properties, which can be quantified and controlled  
107 directly and independently as measured via a drought index. FIND uti-  
108 lizes an iterative optimization technique in which portions of a synthetic  
109 streamflow time series are sampled and replaced at every iteration according  
110 to 5 optimization objectives. These objectives involve reaching the target  
111 drought frequency, intensity, and duration, while also preserving the histor-  
112 ical monthly streamflow autocorrelation and hydrological distribution dur-  
113 ing non-drought periods. FIND utilizes standardized drought indices as a  
114 standardized measure for quantifying drought properties, namely SSI when  
115 generating streamflow scenarios, and the Standardized Precipitation index  
116 (SPI, (McKee et al., 1993)) for precipitation scenarios.

117 FIND can support a variety of applications in water resources systems  
118 analysis. In general, weather generators have long been used to sample hy-  
119 drological variability beyond historical records to create larger datasets for  
120 training and testing water management strategies. Unlike existing gener-  
121 ators, FIND allows targeted sampling of drought frequency, intensity and  
122 duration, making it ideal for evaluating drought planning and management  
123 strategies specifically. Extending drought sampling is particularly impor-  
124 tant as the historical record may only contain a limited number of drought  
125 events, which could lead to overfitting drought strategies to a few drought oc-  
126 currences. Additionally, FIND enables the simulation of non-stationarity in  
127 drought properties, including changes in frequency, intensity, and duration.  
128 This allows users to train and test a system under more severe conditions  
129 than historically observed. Lastly, by systematically assessing a system’s  
130 response to independent changes in drought properties, FIND can support  
131 bottom-up vulnerability analysis whose goal is to draw a clear understand-  
132 ing of the relationship between changes in a specific drought property and  
133 its associated impact.

134 In this work, we demonstrate several FIND applications in hydrologi-  
135 cal time series generation, including sampling streamflow time series with  
136 drought statistics comparable to the historical record, generating streamflow  
137 scenarios for multiple correlated sites while preserving their cross-site cor-  
138 relation, and independently perturbing specific drought properties for bottom-

139 up vulnerability analysis. We showcase these functionalities through exper-  
140 iments conducted on a streamflow location on the Pit River in northern  
141 California. The code developed for these experiments is openly accessible  
142 online and its applicability is intended to extend beyond what presented in  
143 this paper.

144 The remaining sections of the paper are structured as follows. The Meth-  
145 ods section details the calculation of the adopted drought index and drought  
146 characteristics, provides an overview of the FIND algorithm and its objec-  
147 tives. The Case Study section introduces the streamflow sites used in the  
148 analysis, and outlines the experimental design. The Results section presents  
149 the findings of the experiments, and the Conclusion section, discusses the  
150 usability of the tool and highlights potential applications of FIND.

## 151 **2. Methods**

152 This chapter is structured in 5 sections. First, we define quantitative  
153 measures of droughts and their properties by introducing the calculation of a  
154 drought index in section 2.1. Second, we present the FIND algorithm in sec-  
155 tion 2.2. Third, we formulate its objective functions in section 2.3. Fourth,  
156 section 2.4 presents an application of FIND for correlated multisite genera-  
157 tion. Finally, we present the experimental design for this paper’s numerical  
158 analysis.

### 159 *2.1. Quantification of drought characteristics and SSI calculation*

160 Standardized drought indices offer a quantitative and consistent way to  
161 assess drought properties of frequency, intensity, and duration, allowing for  
162 comparisons across different regions and time periods. One widely used  
163 drought index is the Standardized Precipitation Index (SPI), which mea-  
164 sures the deviation of precipitation from its long-term average over a specific  
165 time period (McKee et al., 1993). Similar standardized indices have been  
166 developed for various hydrometeorological variables, including the Standard-  
167 ized Streamflow Index (SSI) also known as Standardized Runoff Index (SRI)  
168 (Vicente-Serrano and López-Moreno, 2005). The experiments contained in  
169 this paper use streamflow data, so we will refer to SSI in the text that follows,  
170 noting that the proposed concepts hold true for SPI as well.

171 The SSI is calculated as follows. First, long-term monthly streamflow  
172 data for a particular location are aggregated over a desired time length,  
173 typically ranging from a few months to a year. A probability distribution

174 function (PDF), such as the Gamma distribution, is selected to model the  
175 data. The parameters of the Gamma distribution are estimated using statisti-  
176 cal methods like the maximum likelihood estimation. Next, the observed  
177 streamflow values are standardized by converting them to standard normal  
178 distribution values based on the estimated Gamma parameters. This trans-  
179 formation allows us to compare the observed streamflow to the long-term  
180 average in terms of standard deviations. The SSI is then calculated for each  
181 month by subtracting the long-term average cumulative distribution function  
182 value from the observed standardized value. The resulting SSI values repre-  
183 sent the standard deviation of the aggregated streamflow from the long-term  
184 average, and they can be positive (indicating wetter conditions) or negative  
185 (indicating drier conditions).

186 Using the SSI time series, it is possible to identify drought events within  
187 the specified time period as a prolonged period of negative SSI whose in-  
188 tensity and duration are higher than a given critical threshold. While some  
189 standard values of these critical thresholds have been proposed, e.g., the Joint  
190 European Commission’s definition of meteorological drought (Spinoni et al.,  
191 2015), they are widely understood to be application specific. In the case of  
192 the FIND algorithm, they can be set by users.

193 More formally, given the SSI time series, we identify a total of  $N_{DE}$   
194 drought events where the  $i_{th}$  drought event is denoted as  $DE_i$ . For  $DE_i$   
195 is classified as drought event if its intensity is higher than the minimum  
196 intensity threshold  $In(DE_i) > In_{min}$ , and its duration is higher than the  
197 minimum duration threshold  $D(DE_i) > D_{min}$ .

198 Specifically, drought intensity  $In(DE_i)$  is measured as the average value of  
199 the SSI time series during the duration of the drought, and drought duration  
200  $D(DE_i)$  refers to the number of months during which a drought persists. A  
201 drought event ends when followed by a wet spell (positive SSI) of a duration  
202 of  $nmonths\_end\_drought$  months.

203 Lastly, the drought frequency  $F(DE)$  in a time series is calculated as the  
204 number of drought occurrences over the time series, divided by its length in  
205 years  $Ny$ .

## 206 2.2. FIND drought generator algorithm

207 FIND is an iterative synthetic streamflow generator where a streamflow  
208 time series is altered over thousands of iterations with Simulated Annealing  
209 (SA, Kirkpatrick et al. (1983)) until it reaches the desired drought properties  
210 while maintaining observed hydrological variability. SA has long been used

211 to solve combinatorial optimization problems in the water resources litera-  
212 ture (Dougherty and Marryott, 1991; Cunha and Sousa, 1999; Thyer et al.,  
213 1999), particularly to reconstruct time series that satisfy specified properties  
214 (Bárdossy, 1998). Each iteration generates a new, *swapped* streamflow time  
215 series by replacing a portion of the original, *parent* time series. The two  
216 series are compared across the optimization objectives of drought frequency,  
217 intensity, duration, monthly autocorrelation, and hydrological distribution  
218 during non-drought periods. One of the two time series is selected to become  
219 the next iteration’s parent time series according to their objective values.  
220 The algorithm proceeds iteratively until a termination criterion is met.

221 Below, we provide more details on each step of the FIND algorithm,  
222 following the schematic in Figure 1.

223 a. **Parameter and time series initialization:** the user selects the tar-  
224 get frequency, intensity, and duration of droughts, either as an absolute  
225 value, or as a fraction of historically observed drought characteristics. In  
226 addition, a number of preset optimization parameters can be adjusted.  
227 These include objective weights, a tolerance parameter that determines  
228 convergence, the initial temperature  $T$  parameter for SA and its decrease  
229 rate, the initial number of consecutive months  $n\_months$  to replace in the  
230 parent time series and its decrease rate. The initial parent time series is  
231 generated by randomly extracting monthly values from historically cal-  
232 ibrated monthly streamflow distributions. The length of the generated  
233 time series is controlled by the parameter  $nyear\_to\_generate$  set to 100  
234 years.

235 b. **Swapped time series generation:** A swapped time series is generated  
236 by replacing a portion of length  $n\_months$  from the parent time series. We  
237 achieve this in 4 steps (Figure 1b.). First, we aggregate historical stream-  
238 flow with a rolling window of  $n\_months$ , obtain the  $n\_months$ -cumulative  
239 historical distribution, and extract a random value from it. This will be  
240 the new cumulative streamflow value for the  $n\_months$  segment for the  
241 swapped time series. Second, we disaggregate the cumulative value to  
242 monthly values using the k-nearest neighbor (k-NN) method (Fix, 1985).  
243 This method searches historical  $n\_months$ -long periods with a cumulative  
244 streamflow value that is closest to the extracted value and applies the  
245 same disaggregation factors to the extracted value. Third, we extract a  
246 random timestamp in the parent time series following which the portion of  
247 length  $n\_months$  is replaced, generating a swapped time series as a fourth

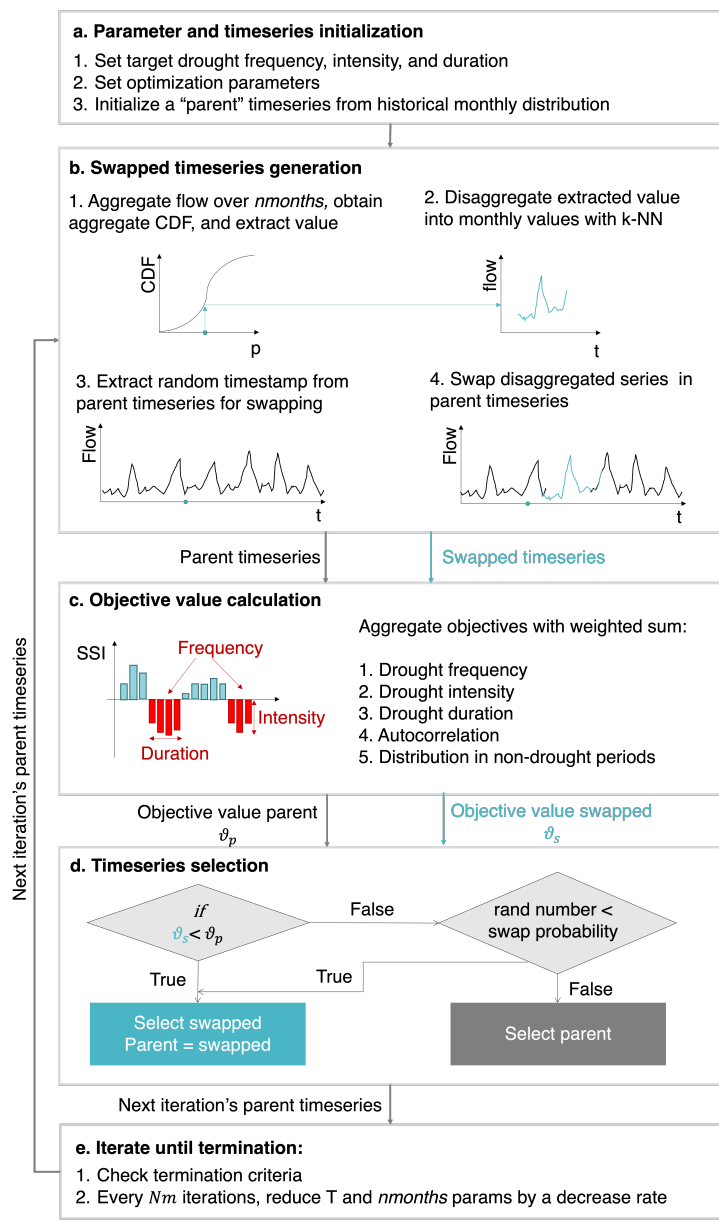


Figure 1: Schematic representation of the 5 steps in the FIND algorithm.



248 step.

249 c. **Objective value calculation:** the aggregate objective value  $\mathcal{J}$  is calcu-  
250 lated for both the parent and swapped time series as a weighted sum of  
251 5 single objective values  $\mathbf{J}_i$ . The single objectives include the time series'  
252 deviation from the target frequency, intensity, duration, monthly autocor-  
253 relation over a 12-month period, and the 25th, 50th, and 75th percentiles  
254 during non-drought periods. The mathematical formulation of each ob-  
255 jective is presented in section 2.3. The aggregated objective represents  
256 a measure of distance between the desired streamflow characteristics and  
257 those of the current time series, and lower values are preferred.

d. **time series selection:** A time series is selected between the parent and  
swapped to become the new parent time series for the next iteration.  
According to SA selection principles, if the swapped time series has a lower  
(better) objective value, the swapped time series becomes the new parent.  
If the parent time series has lower objective, the algorithm can occasionally  
select non-improving swaps with a probability  $pmov$  determined by the  
ratio between the parent and swapped aggregate objective values  $\mathcal{J}_p$  and  
 $\mathcal{J}_s$  respectively, and the temperature parameter  $T$ :

$$pmov = \left| \exp \left( \frac{\mathcal{J}_p - \mathcal{J}_s}{\mathcal{J}_p} * T \right) \right| \quad (1)$$

258 SA has been demonstrated to be more resistant than regular greedy se-  
259 lections (i.e., strictly minimizing the objective value) in escaping local  
260 minima (Dougherty and Marrayott, 1991; Borgomeo et al., 2015a).

261 e. **Iterate until termination:** the time series selected during the previ-  
262 ous step becomes the new parent time series. The algorithm proceeds  
263 by iterating through steps b.-e. until one of the two terminating criteria  
264 is met, namely the parent time series aggregated objective is lower than  
265 a tolerance parameter  $\mathcal{J}_p < tol$ , or the maximum Number of Function  
266 Evaluations NFE is reached. NFE depends on 2 user-defined parameters,  
267 as typical in SA applications:  $NFE = m * Nm$ , where  $m$  is the num-  
268 ber of temperature drops, and  $Nm$ , is the number of iterations for each  
269 temperature. In FIND, both of temperature and  $n\_months$  are lowered  
270 every  $Nm$  iterations by a fraction determined by the decrease rate  $DR$ ,  
271 where  $0 < DR < 1$ . The rationale of the parameter change is that as the  
272 optimization proceeds, the search can move from a larger *exploration* of  
273 the optimization space to a more targeted *exploitation*, or refinement, of  
274 the current solution.

275 The FIND algorithm draws inspiration from a synthetic streamflow gener-  
 276 ator introduced by Borgomeo et al. (2015a), which also uses SA to iteratively  
 277 swap values in an initialized synthetic streamflow time series. However, there  
 278 are significant differences between the two methods. The previous generator  
 279 swaps the position of two elements in the synthetic time series during each  
 280 iteration, restricting the reorganization to values that are already present in  
 281 the synthetic series, and allowing to swap only two values at a time. FIND,  
 282 instead, can replace portions of varying length in the time series, allowing  
 283 us to more efficiently explore the optimization space. In addition, the new  
 284 swapped values are extracted from a calibrated distribution rather than from  
 285 a different portion of the same series. This is critical when trying to generate  
 286 a synthetic time series with, for instance, longer or more intense droughts,  
 287 as it can happen that no recombination of the initialized time series values  
 288 can achieve the desired drought properties. Furthermore, FIND introduces  
 289 the calculation of drought indices in the optimization and employs different  
 290 objective functions that focus on controlling drought properties rather than  
 291 streamflow time series statistics.

### 292 *2.3. Objective calculation*

293 In this section, we formulate the objective functions calculated at step  
 294 4 of the FIND algorithm. The 5 single objectives considered in this algo-  
 295 rithm are the deviation from target frequency, intensity, duration, observed  
 296 monthly autocorrelation, and observed non-drought periods quartiles. Only  
 297 one objective, the autocorrelation, is calculated directly on the streamflow  
 298 time series while the other 4 are calculated on the relative SSI index time  
 299 series. In FIND, the SSI of a synthetic streamflow time series is always cal-  
 300 culated with reference to historical long-term averages rather than synthetic  
 301 averages. This allows to maintain comparability across different synthetic  
 302 time series as well as relevance for the site of interest.

- Drought frequency deviation: defined as the deviation between the target drought frequency  $F_T$  and the drought frequency obtained in the synthetic time series. Because all the time series generated in the code have the same length of  $N_y = 100$  years, for simplicity we define the frequency objective directly on the number of drought events, rather than their frequency over the 100-year period.

$$J_F = |N_{DE} - F_T| \quad (2)$$

- Drought intensity deviation: defined as the average difference between the intensity of each drought event  $In(DE_i)$  and the target intensity  $In_T$ , plus the difference between the average drought intensity and the target. The last element is added to penalize biased deviation, for instance in the case that the intensity of all generated drought events is lower than the target.

$$J_{In} = \sum_{i=1}^{N_{DE}} |In(DE_i) - In_T| + \left| \frac{\sum_{i=1}^{N_{DE}} In(DE_i)}{N_{DE}} - In_T \right| \quad (3)$$

- Drought duration deviation: analogously to the intensity objective, it is defined as the average difference between the duration of each drought event  $D(DE_i)$  and the target duration  $D_T$ , plus the difference between the average drought duration and the target.

$$J_D = \sum_{i=1}^{N_{DE}} |D(DE_i) - D_T| + \left| \frac{\sum_{i=1}^{N_{DE}} D(DE_i)}{N_{DE}} - D_T \right| \quad (4)$$

- 303 • Autocorrelation deviation: this objective penalizes the deviation between the 12-month intermonthly autocorrelation between the historical time series and the synthetic one. The duration of 12 months is chosen with the aim of preserving in-year autocorrelation as well as year-to-year autocorrelation (Herman et al., 2016).

308 For a generic time series  $y$ , the autocorrelation value for a lag time  $k$  is the correlation between values that are  $k$  time periods apart:  $Corr(y_t, y_{t-k})$ . As follows, the monthly autocorrelogram is the array of autocorrelation values from lag time 1 to 12 as in  $AC = [Corr(y_t, y_{t-k})]$  for  $k = 1, 2, \dots, 12$ .

We call the 12-month autocorrelogram calculated on the historically observed time series as target autocorrelogram  $AC_T$ , and the synthetic time series' as  $AC_{synt}$ . Finally, the objective value  $J_{AC}$  is calculated as the sum of deviations between the two autocorrelogram series at each lag time.

$$J_{AC} = \sum_{k=1}^{12} |AC_{synt} - AC_T| \quad (5)$$

313 • non-drought quartiles deviation: defined as the summed deviation be-  
 314 tween the 25th, 50th, and 75th percentiles calculated for the historical  
 315 SSI and the synthetic time series in non-drought periods. This objective  
 316 aims to preserve historical hydrological distribution during non-drought  
 317 periods even when the drought properties are modified. Non-drought  
 318 events *nde* are here defined as the entire time series  $t = 1 : H$  except  
 319 the time segments occupied by drought events. The objective is thus  
 320 formulated as:

$$\begin{aligned}
 J_{NDE} = & |q25_{nde} - q25_T| + \\
 & |q50_{nde} - q50_T| + \\
 & |q75_{nde} - q75_T|
 \end{aligned} \tag{6}$$

321 where  $q25_{nde}$  is the synthetic time series 25th percentile during non-  
 322 drought periods, and  $q25_T$  is the historical target percentile value, with  
 323 analogous notations for the 50th and 75th percentiles.

324 Finally, the aggregated objective  $\mathcal{J}$  for a time series is the weighted sum  
 325 of the 5 single objectives with a convex user-defined set of weights  $\omega_i$ .

$$\mathcal{J} = \omega_1 * J_F + \omega_2 * J_{In} + \omega_3 * J_D + \omega_3 * J_{AC} + \omega_5 * J_{NDE} \tag{7}$$

326 Although it is not strictly necessary, in FIND's software the duration  
 327 objective is divided by a factor of 100 in order to align its order of magni-  
 328 tude to that of the other objectives. We find that this choice simplifies the  
 329 identification of a suitable set of weights for the problem.

#### 330 2.4. Multisite generation

331 In this section, we present the method used by FIND to generate synthetic  
 332 scenarios for multiple sites while preserving the correlation between the sites'  
 333 hydrological conditions, represented by the SSI values. We prioritize the  
 334 correlation between SSI indices, rather than streamflow, to more accurately  
 335 propagate drought conditions across correlated sites.

The algorithm employed for this analysis differs from the one described in  
 Section 2.2 only for the objective function used. In this case, the objective is  
 to minimize the deviation between the cumulative squared dispersion of the  
 SSI values for the two sites  $s1$  and  $s2$  and the target dispersion  $Dis_T$ . The

target dispersion is defined as the historically observed SSI squared dispersion for the two sites, ensuring that the synthetic scenarios closely align with the historical data:

$$Dis_T = \sum_{t=1}^H (SSI_{s1_H} - SSI_{s2_H})^2 \quad (8)$$

336 First, FIND generates a synthetic streamflow scenario and the relative  
 337 SSI time series for site 1  $SSI_{s1}$  using the algorithm presented in section  
 338 2.2. Then, FIND generates the correlated streamflow scenario for site 2 by  
 339 iterative recombining a randomly sampled streamflow time series for the site,  
 340 until matching the dispersion between  $SSI_{s1}$  and  $SSI_{s2}$  with the target  $Dis_T$   
 341 . The objective function is formulated as:

$$\mathcal{J}_{Dis} = \left| \sum_{t=1}^H (SSI_{s1} - SSI_{s2})^2 - Dis_T \right| \quad (9)$$

### 342 2.5. Use cases and Experiments

343 FIND is a versatile tool that supports hydrological time series generation  
 344 for multiple purposes, including sampling hydrological variability beyond the  
 345 historical record, generating correlated multi-site scenarios, and perturbing  
 346 specific hydrological characteristics for bottom-up vulnerability analysis. In  
 347 this paper, we demonstrate FIND’s suitability for each of these objectives in  
 348 three experiments.

349 In the first experiment, we utilize FIND to sample historical drought  
 350 variability beyond the observed record. Our goal is to generate synthetic  
 351 streamflow time series that exhibit comparable drought properties to the  
 352 historical data while maintaining the site’s historical temporal properties  
 353 (monthly autocorrelation) and hydrological distribution during non-drought  
 354 periods. In follow-up studies, these scenarios may be used to augment the  
 355 sample of historical droughts with synthetic droughts within a similar range  
 356 of frequency, intensity, and duration. A larger drought sample may be used  
 357 to more robustly assess the system’s response to droughts and the efficacy of  
 358 drought mitigation policies.

359 The second experiment demonstrates FIND’s ability to generate synthetic  
 360 scenarios for two sites with correlated hydrology. Water resources planning  
 361 often involves modeling a spatial extent, such as a watershed, that contains  
 362 multiple sites of interest. These sites may include, for instance, multiple cor-  
 363 related inflow points to one or more reservoirs, or upstream and downstream

364 flows. FIND allows to generate streamflow scenarios for multiple sites while  
365 preserving the cross-site correlation of hydrological characteristics.

366 Lastly, synthetic streamflow generators are used in bottom-up vulnera-  
367 bility analysis studies where relevant hydrological properties are perturbed  
368 to simulate plausible climate change effects and assess system vulnerability  
369 to these changes. FIND is the first tool capable of directly and independ-  
370 dently controlling drought frequency, intensity, and duration in generated  
371 streamflow time series thus enabling future bottom up vulnerability studies  
372 to related changes in drought conditions to vulnerability outcomes. In exper-  
373 iment 3, we demonstrate this capability by running the algorithm 25 times  
374 intersecting 5 increments of the drought duration and intensity properties,  
375 and generating a wide range of drought conditions for the site of interest.

376 Each experiment requires manual tuning of FIND’s optimization param-  
377 eters, including objective weights for experiments 1 and 3, and termination  
378 criteria. Tuning objective weights is often required in single-objective op-  
379 timization algorithms like SA to convert multiple objectives into a single  
380 aggregate objective function. By tuning these parameters, the modeler tries  
381 to achieve the desired tradeoff between multiple objectives by adjusting their  
382 scale and importance. The tuning of termination criteria balances computa-  
383 tional time and desired performance.

384 The appropriate parameterization depends on the characteristics of the  
385 historical record for the case study and the specific goal of hydrological time  
386 series generation, as illustrated in the examples above. In the next section,  
387 we provide details on the case study adopted for the experiments in this  
388 paper and the parameterizations applied to each experiment.

### 389 **3. Case study**

390 This study examines two sites along the Pit River in northeastern Califor-  
391 nia. The Pit River is a major river that drains from northeastern California  
392 into the state’s Central Valley crossing the Cascade Range. It is the longest  
393 tributary of the Sacramento River and contributes up to eighty percent of  
394 the combined water volume into the Shasta Lake reservoir.

395 The selected sites are located approximately 100 miles apart in the towns  
396 of Big Bend and Candy, where long-running USGS monitoring stations have  
397 collected Pit river flow data for decades. The analysis of this paper focus on  
398 the Big Bend site, utilizing the unimpaired monthly flow record from May  
399 1944 to June 2022. The Candy site, located northeast of Big Bend along

400 the Pit River, is only used in experiment 2 to demonstrate the algorithm’s  
401 capability to generate streamflow scenarios for multiple sites while preserving  
402 cross-site correlation. It is important to note that these two sites were chosen  
403 for demonstrative purposes, and the software is designed to accommodate any  
404 monthly streamflow or precipitation time series uploaded by the user, as long  
405 as the recorded time series is long enough to capture hydrological trends and  
406 variability. Generally, an historical record of at least 30 years is necessary,  
407 and 50 years is recommended (McKee et al., 1993).

408 To demonstrate FIND’s versatility and usability with precipitation data,  
409 the SI reports the same experiments shown in the main paper, but for  
410 monthly precipitation data rather than streamflow data. The main pre-  
411 cipitation site is located in Santa Rosa, CA, and the secondary site for the  
412 multisite experiment is the neighboring Fort Ross.

### 413 3.1. *Experimental parameters*

414 Table 1 summarizes FIND parameters and their adopted values for each  
415 experiment.

416 The first set of parameters is the drought threshold. Their selection de-  
417 pends on the goal of the application at hand. For instance, some applications  
418 may focus on capturing only the most severe droughts to inform emergency  
419 drought planning strategies, while other applications might want to capture  
420 many different dry spells to devise a routine drought management strategy.

421 Second, the selection of the optimization parameters depends on the com-  
422 plexity and features of the optimization problem. In general, low values of  
423  $n\_months$  and  $T$  allow small targeted improvements of the time series rather  
424 than large-scale exploration of the optimization space. Setting low values for  
425 these parameters may therefore expose to local minima traps. Conversely,  
426 high values of  $n\_months$  and  $T$  allow large-scale exploration of the space  
427 but hinder the fine-tuning, or "exploitation", of solutions, potentially slow-  
428 ing down convergence significantly. The parameter  $DR$  controls the rate  
429 at which the values of  $n\_months$  and  $T$  decrease during the optimization  
430 managing the transition between the initial exploration phase and the fi-  
431 nal exploitation phase. Parameters  $Nm$ ,  $m$ , and  $tol$  control the termination  
432 criteria and are selected to balance computational time and final objective  
433 value.

434 Lastly, optimization weights are selected to allow the optimization process  
435 to appropriately prioritize specific objectives based on the context and re-  
436 quirements of the application. For instance, in Experiment 3, where drought

437 intensity and duration are perturbed with respect to historical observations,  
 438 achieving good performance requires assigning higher weights to intensity  
 439 and duration objectives compared to Experiment 1, which only replicates  
 440 historical droughts.

	Parameter	Explanation	Exp 1	Exp 2	Exp 3
drought thresholds	$D_{min}$	minimum drought duration in months	24	24	24
	$I_{n_{min}}$	minimum drought intensity	-0.5	-0.5	-0.5
optimization parameters	$n_{months}$	initial number of months replaced at each iteration	48	48	60
	$T$	initial SA temperature	0.001	0.001	0.001
	$DR$	decrease rate for parameters $n_{month}$ and $T$	0.8	0.8	0.8
	$Nm$	iterations for each $T$ and $n_{month}$ state	600	600	1000
	$m$	number of $T$ and $n_{month}$ changes	15	15	15
	$tol$	optimization stops when objective is lower than $tol$	0.02	0.02	0.005
optimization weights	$\omega_1$	intensity weight	0.1		0.1
	$\omega_2$	duration weight	0.4		0.6
	$\omega_3$	frequency weight	0.1		0.1
	$\omega_4$	autocorrelation weight	0.2		0.1
	$\omega_5$	non-drought distribution weight	0.2		0.1
	$W$	dispersion weight for multisite experiment		1	

Table 1: FIND parameters and adopted parameterization for each experiment.

## 441 4. Results

442 This chapter presents the results of the three experiments discussed in  
 443 Section 2.5. In the first experiment, we use FIND to sample drought vari-  
 444 ability beyond the historical record.

445 For this experiment, we generate 10 synthetic time series for the Big Bend  
 446 streamflow site (Figure 2). Panel a. displays the historical streamflow time  
 447 series in green, and the SSI computed for the site with 12-month rolling time  
 448 window, highlighting the three identified historical droughts in red. The  
 449 average observed drought intensity is equal to -0.88, the drought duration is  
 450 55.6 months or 4.6 years, and the frequency is 3 drought events in 78 years,  
 451 which equals one drought every 26 years.

452 We plotted the streamflow and SSI time series for one of the generated  
 453 synthetic scenarios (Figure b). An interactive version of this figure is available  
 454 on GitHub (see code availability section), allowing users to browse through  
 455 the 10 series. Panels a. and b. have been rescaled to have comparable  
 456 spacing on the horizontal axis, as the historical time series spans 78 years  
 457 while the generated time series span 100 years. Lastly, panel c. illustrates  
 458 the median and quartiles for each month of the year of the historical and



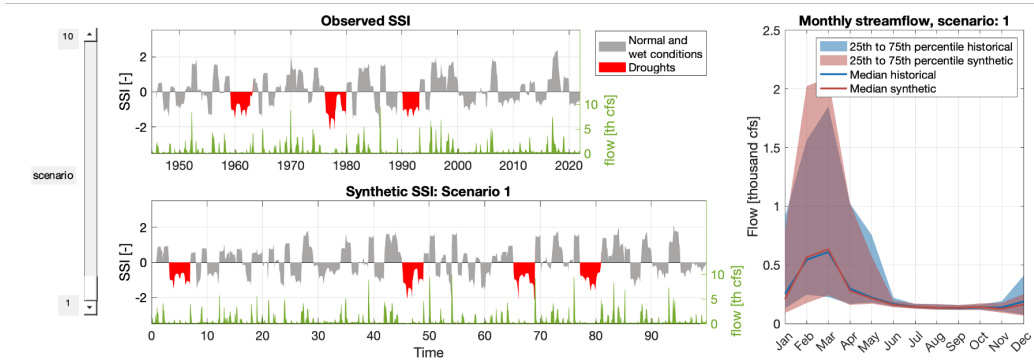


Figure 2: Synthetic drought scenario generated for the Big Bend streamflow site along the Pit River. Panel a: observed streamflow time series, and SSI drought index calculated on observed streamflow. Three droughts are identified according to the parameters defined in section 3.1. Panel b: one of the generated synthetic streamflow scenario and its relative SSI time series. Panel c. monthly median and quartiles of historical and synthetic streamflow series. An interactive version of this figure that allows to move the slider on the left is available on GitHub.

459 synthetic streamflow series, demonstrating a good overlap between historic  
 460 and simulated data, and confirming the preservation of expected hydrological  
 461 properties.

462 Figure 3 validates the observations made in Figure 2 by presenting the  
 463 performance of the 10 generated scenarios across five optimization objec-  
 464 tives: drought intensity, duration, frequency, monthly autocorrelation, and  
 465 quartiles during non-drought periods. Panels a. and b. showcase the inten-  
 466 sity and duration of drought events in the scenarios (red) compared to the  
 467 historical scenario (blue). FIND successfully generates drought events with  
 468 intensities and durations that are comparable in magnitude and range to  
 469 historical droughts. Panel c. shows the desired drought frequency through a  
 470 barplot. Historically, we observed 3 droughts in 78 years, which we approxi-  
 471 mate to a frequency of 4 droughts in 100 years, the length of the generated  
 472 scenarios. The autocorrelogram in panel d. displays the 24-month stream-  
 473 flow autocorrelation of the synthetic scenarios in red alongside the historical  
 474 streamflow (blue), serving as the target. We note a slight underestimation of  
 475 the synthetic autocorrelation at a lag time of 1 month but overall, the syn-  
 476 thetic series performs well in capturing the historical time structure. Lastly,  
 477 panel e. presents the 25th, 50th, and 75th percentiles of the SSI index dur-  
 478 ing non-drought periods. In this case as well, the algorithm demonstrates its

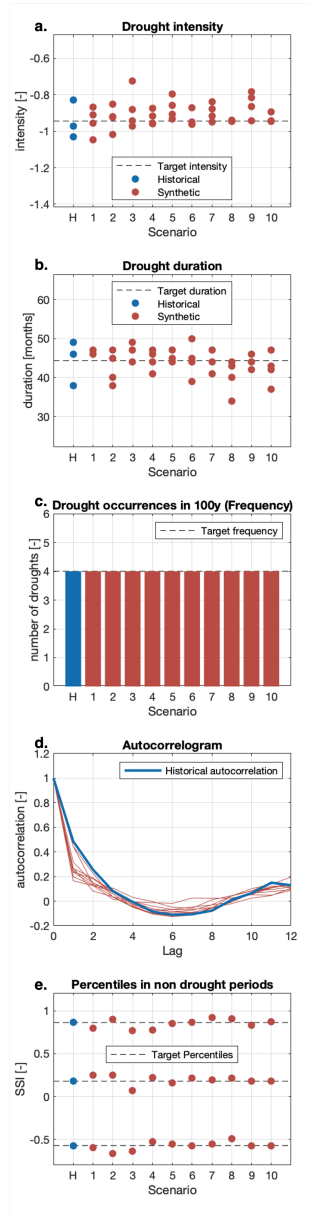


Figure 3: Visualization of the performance across the 5 objectives of the 10 generated scenarios (red) alongside historical observation (blue). Panel a: drought intensity, b: duration, c: frequency, d: autocorrelation, and e: percentiles during non-drought periods.

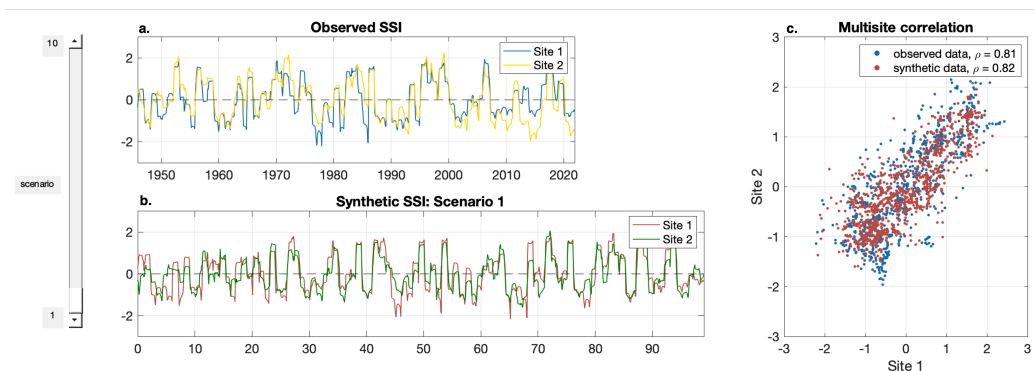


Figure 4: Synthetic drought scenarios generated for two correlated sites along the Pit River, namely Big Bend (site 1) and Canby (site 2). Panel a: SSI drought index calculated on observed streamflow for the two sites. Panel b: SSI time series for a pair of synthetic scenarios for the 2 sites. Visually, they display a similar correlation as the observations. Panel c: scatterplot of the two time series to display their correlation. The cloud of points for the observed and synthetic scenarios overlap, indicating a similar cross-site correlation. An interactive version of this figure that allows to move the slider on the left is available on GitHub.

479 ability to adequately reproduce historical statistics.

480 Figure 4 presents the results of experiment 2, which focuses on correlated  
 481 multisite streamflow generation. Panel a. shows the historical SSI for the  
 482 two sites, namely Big Bend and Canby. The correlation between the sites  
 483 is visualized in the scatterplot of panel c, where the cloud of blue dots is  
 484 distributed along the main diagonal, indicating the a positive correlation.  
 485 Panel b. shows one SSI scenario generated in the previous exercise in red,  
 486 alongside the relative correlated synthetic SSI for site 2. The red dots in  
 487 panel c demonstrate that the synthetic data presents a similar dispersion as  
 488 the historically observed data. The interactive version of this figure, avail-  
 489 able on GitHub, enables users to browse through the 10 generated scenarios,  
 490 providing a more comprehensive exploration of the results.

491 In the third experiment, illustrated in Figure 5, we demonstrate FIND's  
 492 capability to generate synthetic streamflow scenarios with user-specified drought  
 493 properties, distinct from the historical record. This use mode is particularly  
 494 valuable for future bottom-up vulnerability analysis that aim to quantify the  
 495 vulnerability outcomes of specific climate changes in drought properties. It's  
 496 important to note that in experiment 1, our focus was on generating droughts  
 497 that captured the magnitude and range of historical events. However, in this

498 experiment, our goal is to generate droughts that closely align with a specific  
499 target of interest, emphasizing a narrow range over historical range. This  
500 targeted approach is more suitable to a vulnerability analysis whose goal is  
501 to draw a clear understanding of the relationship between a specific drought  
502 property and its associated impact.

503 The proposed experiment focuses on changes in drought intensity (vertical  
504 axis in Figure 5a. ) and duration (horizontal axis). We consider change  
505 factors ranging from 0.75 (representing a 25% decrease from the historical  
506 average) to 1.75 (representing a 75% increase), with increments of 25%. The  
507 top axis and right axes represent change factors of duration and intensity,  
508 respectively, while the left and bottom axes display the absolute values of  
509 duration and intensity. Within each square, a small white dot represents the  
510 target for each generated drought, with the square delimiting a 12.5% (half  
511 of an increment) deviation around the target multiplier.

512 For this figure, we generated three drought scenarios for each combination  
513 of duration and intensity. Each scenario contains three drought occurrences,  
514 represented by dots in the duration-intensity space. The color of each dot  
515 corresponds to the combination of duration and intensity for which the sce-  
516 nario was generated: green to yellow shades indicate increasing intensity,  
517 while dark to light shades indicate increasing duration. Dots located within  
518 squares of the same color indicate that the corresponding drought scenario  
519 aligns with the desired characteristics of duration and intensity within a nar-  
520 row range. This holds true for 97% of the generated droughts (218 out of 225  
521 generated), indicating a high level of success. The few exceptions, located  
522 near the boundaries of the target squares, can still be considered within an  
523 acceptable range.

524 Panels b. and c. show examples of generated SSI and streamflow time  
525 series for different drought properties. We show Short intense droughts in  
526 panel b., namely the intensity-duration combination in the bottom-left of the  
527 matrix, which corresponds to high intensity (+75% with respect to histori-  
528 cal), and low duration (-25% with respect to historical). In panel c., we shows  
529 examples of Long mild droughts, with long duration (+75% with respect to  
530 historical) and low intensity (-25% with respect to historical).

## 531 5. Conclusions and usability

532 This study presents FIND (Frequency, INtensity, and Duration) drought  
533 generator, the first synthetic streamflow and precipitation generator that

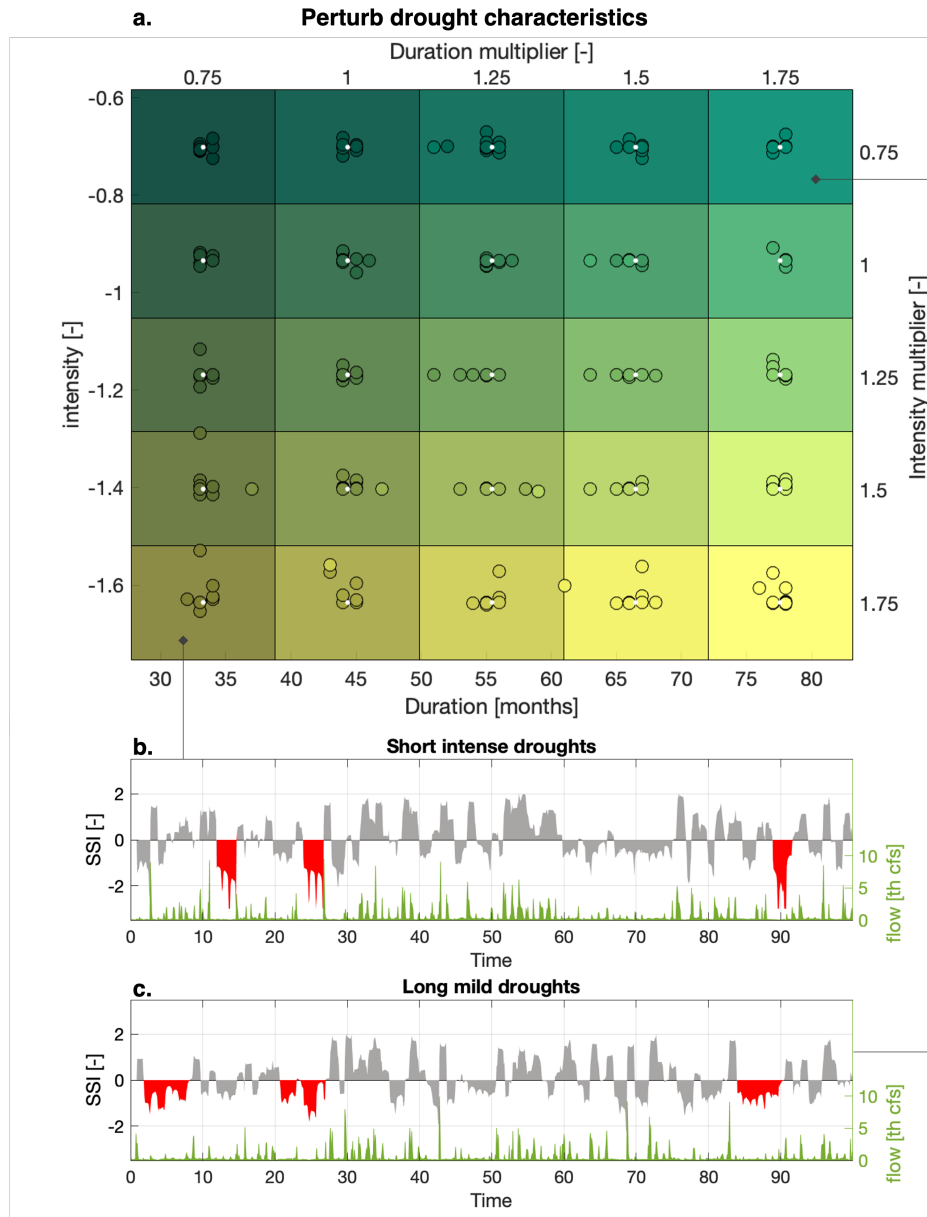


Figure 5: Panel a. Three drought scenarios including 3 drought each are generated for 25 different increments of target intensity and duration and plotted in the space of drought intensity (vertical axes) and duration (horizontal axes). The white dots indicate the targets, and are located in a square delineating a narrow range around the target amounting to half a target increment. Each colored dot represents a single drought in a drought scenario. Dots that match their background color are located in a narrow range of the target duration and intensity they were designed for, indicating success. Panel b. shows one of the generated scenarios for the combination of drought properties in the bottom-left of the matrix, namely the Short intense droughts, with high intensity (+75% with respect to historical), and low duration (-25% with respect to historical). Panel c. shows one of the generated scenarios for the combination of drought properties in the top-right of the matrix, namely Long mild droughts, with long duration (+75% with respect to historical) and low intensity (-25% with respect to historical).

534 allows users to control the drought properties of a synthetic streamflow sce-  
535 nario directly and independently. This advances current synthetic generation  
536 capabilities as existing methods only allow perturbation of statistics of hydro-  
537 climatological time series, which are indirectly linked to drought properties,  
538 rather than directly controlling drought properties. It is therefore the first  
539 synthetic streamflow generator that enables bottom-up vulnerability stud-  
540 ies to explicitly relate changes in drought properties to system vulnerability  
541 outcomes.

542 FIND is designed to support water resources systems analysis applica-  
543 tions that seek to train and test drought planning and management strate-  
544 gies under historical and plausible future drought conditions by augmenting  
545 the available sample of drought events. Varying drought frequency, inten-  
546 sity, and duration directly and independently allows modelers to identify the  
547 drought characteristics that pose the greatest threat to water systems. For  
548 example, previous work in Santa Barbara, CA found that drought intensity,  
549 not duration or frequency, led to the greater water supply deficits (Zan-  
550 iolo et al., 2023). This insight, which cannot be achieved with a traditional  
551 streamflow generator, can be used by planners to design drought manage-  
552 ment approaches that target the types of droughts that pose the greatest  
553 threats.

554 We demonstrate FIND’s applicability to a series of tasks, including sam-  
555 pling hydrological variability beyond the historical record, generating corre-  
556 lated multi-site scenarios, and perturbing specific drought characteristics for  
557 bottom-up vulnerability analysis a streamflow site in northeastern Califor-  
558 nia. Beyond the applications demonstrated in this paper, FIND is intended  
559 to be a tool freely shared with the community for a variety of hydrological  
560 generation problems. In addition to streamflow scenarios, FIND can also be  
561 applied to the generation of monthly precipitation scenarios as shown in the  
562 SI, with no modification to the code.

563 Anyone interested in using FIND can freely download the open-source  
564 code from a GitHub repository and follow the instructions in the README  
565 file which provides guidance on loading the streamflow or precipitation record  
566 of interest, and tuning some application-specific parameters. In our experi-  
567 ence, a few attempts are needed to tune the set of objective weights that  
568 balance the 5 optimization objectives adequately for a new case study, but  
569 future work can extend FIND to include techniques to automatically tune  
570 weights and other optimization parameters.

## 571 **Appendix A. Code Availability**

572 The open-source code developed for these experiments is made available  
573 on an online repository at <https://github.com/m-zaniolo/FIND-drought-generator>.  
574 FIND runs on recent Matlab installations (2021 and beyond).

## 575 **Appendix B. Acknowledgment**

576 This work is supported by the National Alliance for Water Innovation  
577 (NAWI), funded by the U.S. Department of Energy, Energy Efficiency and  
578 Renewable Energy Office, Advanced Manufacturing Office under Funding  
579 Opportunity Announcement DE-FOA-0001905. The views expressed herein  
580 do not necessarily represent the views of the U.S. Department of Energy or  
581 the United States Government. We thank Matteo Giuliani for assistance  
582 with beta testing of the published code.

## 583 **References**

- 584 Aadhar, S., Mishra, V., 2020. Increased drought risk in south asia under  
585 warming climate: Implications of uncertainty in potential evapotranspira-  
586 tion estimates. *Journal of Hydrometeorology* 21, 2979–2996.
- 587 Bárdossy, A., 1998. Generating precipitation time series using simulated  
588 annealing. *Water Resources Research* 34, 1737–1744.
- 589 Borgomeo, E., Farmer, C.L., Hall, J.W., 2015a. Numerical rivers: A synthetic  
590 streamflow generator for water resources vulnerability assessments. *Water*  
591 *Resources Research* 51, 5382–5405.
- 592 Borgomeo, E., Pflug, G., Hall, J.W., Hochrainer-Stigler, S., 2015b. As-  
593 sessing water resource system vulnerability to unprecedented hydrological  
594 drought using copulas to characterize drought duration and deficit. *Water*  
595 *Resources Research* 51, 8927–8948.
- 596 Breinl, K., Turkington, T., Stowasser, M., 2015. Simulating daily precip-  
597 itation and temperature: a weather generation framework for assessing  
598 hydrometeorological hazards. *Meteorological Applications* 22, 334–347.
- 599 Brown, C., Ghile, Y., Lavery, M., Li, K., 2012. Decision scaling: Link-  
600 ing bottom-up vulnerability analysis with climate projections in the water  
601 sector. *Water Resources Research* 48.

- 602 Bryant, B.P., Lempert, R.J., 2010. Thinking inside the box: A participatory,  
603 computer-assisted approach to scenario discovery. *Technological Forecasting and Social Change* 77, 34–49.  
604
- 605 Cunha, M.d.C., Sousa, J., 1999. Water distribution network design optimization: simulated annealing approach. *Journal of water resources planning and management* 125, 215–221.  
606  
607
- 608 Dougherty, D.E., Marryott, R.A., 1991. Optimal groundwater management: 1. simulated annealing. *Water Resources Research* 27, 2493–2508.  
609
- 610 Fix, E., 1985. Discriminatory analysis: nonparametric discrimination, consistency properties. volume 1. USAF school of Aviation Medicine.  
611
- 612 Fletcher, S.M., Zaniolo, M., Zhang, M., 2023. Climate oscillation impacts on water supply augmentation planning. *Proceedings of the National Academy of Sciences* 118, e2022196118. doi:10.1073/pnas.2215681120.  
613  
614
- 615 Giuliani, M., Zaniolo, M., Sinclair, S., Micotti, M., Van Orshoven, J., Burlando, P., Castelletti, A., 2022. Participatory design of robust and sustainable development pathways in the omo-turkana river basin. *Journal of Hydrology: Regional Studies* 41, 101116.  
616  
617  
618
- 619 Hall, J., Borgomeo, E., 2013. Risk-based principles for defining and managing water security. *Philosophical Transactions of the Royal Society A: Mathematical, Physical and Engineering Sciences* 371, 20120407.  
620  
621
- 622 Herman, J.D., Reed, P.M., Zeff, H.B., Characklis, G.W., 2015. How should robustness be defined for water systems planning under change? *Journal of Water Resources Planning and Management* 141, 04015012.  
623  
624
- 625 Herman, J.D., Zeff, H.B., Lamontagne, J.R., Reed, P.M., Characklis, G.W., 2016. Synthetic drought scenario generation to support bottom-up water supply vulnerability assessments. *Journal of Water Resources Planning and Management* 142, 04016050.  
626  
627  
628
- 629 de Jager, A., Corbane, C., Szabo, F., 2022. Recent developments in some long-term drought drivers. *Climate* 10, 31.  
630
- 631 Johnson, F., Westra, S., Sharma, A., Pitman, A.J., 2011. An assessment of gcm skill in simulating persistence across multiple time scales. *Journal of Climate* 24, 3609–3623.  
632  
633



- 634 Kirkpatrick, S., Gelatt Jr, C.D., Vecchi, M.P., 1983. Optimization by simu-  
635 lated annealing. *science* 220, 671–680.
- 636 McKee, T.B., Doesken, N.J., Kleist, J., et al., 1993. The relationship of  
637 drought frequency and duration to time scales, in: *Proceedings of the 8th*  
638 *Conference on Applied Climatology*, Boston. pp. 179–183.
- 639 Naumann, G., Alfieri, L., Wyser, K., Mentaschi, L., Betts, R., Carrao, H.,  
640 Spinoni, J., Vogt, J., Feyen, L., 2018. Global changes in drought conditions  
641 under different levels of warming. *Geophysical Research Letters* 45, 3285–  
642 3296.
- 643 Nazemi, A., Zaerpour, M., Hassanzadeh, E., 2020. Uncertainty in bottom-up  
644 vulnerability assessments of water supply systems due to regional stream-  
645 flow generation under changing conditions. *Journal of Water Resources*  
646 *Planning and Management* 146, 04019071.
- 647 Quinn, J.D., Reed, P.M., Giuliani, M., Castelletti, A., Oyler, J.W., Nicholas,  
648 R.E., 2018. Exploring how changing monsoonal dynamics and human  
649 pressures challenge multireservoir management for flood protection, hy-  
650 dropower production, and agricultural water supply. *Water Resources Re-*  
651 *search* 54, 4638–4662.
- 652 Ray, P.A., Bonzanigo, L., Wi, S., Yang, Y.C.E., Karki, P., Garcia, L.E.,  
653 Rodriguez, D.J., Brown, C.M., 2018. Multidimensional stress test for hy-  
654 dropower investments facing climate, geophysical and financial uncertainty.  
655 *Global Environmental Change* 48, 168–181.
- 656 Rocheta, E., Sugiyanto, M., Johnson, F., Evans, J., Sharma, A., 2014. How  
657 well do general circulation models represent low-frequency rainfall variabil-  
658 ity? *Water Resources Research* 50, 2108–2123.
- 659 Singh, J., Ashfaq, M., Skinner, C.B., Anderson, W.B., Mishra, V., Singh, D.,  
660 2022. Enhanced risk of concurrent regional droughts with increased enso  
661 variability and warming. *Nature Climate Change* 12, 163–170.
- 662 Spinoni, J., Naumann, G., Vogt, J., Barbosa, P., 2015. European drought  
663 climatologies and trends based on a multi-indicator approach. *Global and*  
664 *Planetary Change* 127, 50–57.

- 665 Stainforth, D.A., Downing, T.E., Washington, R., Lopez, A., New, M., 2007.  
666 Issues in the interpretation of climate model ensembles to inform decisions.  
667 Philosophical Transactions of the Royal Society A: Mathematical, Physical  
668 and Engineering Sciences 365, 2163–2177.
- 669 Steinschneider, S., Brown, C., 2013. A semiparametric multivariate, multisite  
670 weather generator with low-frequency variability for use in climate risk  
671 assessments. *Water resources research* 49, 7205–7220.
- 672 Tallaksen, L.M., Stahl, K., 2014. Spatial and temporal patterns of large-  
673 scale droughts in europe: Model dispersion and performance. *Geophysical  
674 Research Letters* 41, 429–434.
- 675 Thyer, M., Kuczera, G., Bates, B.C., 1999. Probabilistic optimization for  
676 conceptual rainfall-runoff models: A comparison of the shuffled complex  
677 evolution and simulated annealing algorithms. *Water Resources Research*  
678 35, 767–773.
- 679 Ullrich, S.L., Hegnauer, M., Nguyen, D.V., Merz, B., Kwadijk, J., Vorogushyn,  
680 S., 2021. Comparative evaluation of two types of stochastic  
681 weather generators for synthetic precipitation in the rhine basin. *Journal  
682 of Hydrology* 601, 126544.
- 683 Vicente-Serrano, S.M., López-Moreno, J.I., 2005. Hydrological response to  
684 different time scales of climatological drought: an evaluation of the stan-  
685 dardized precipitation index in a mountainous mediterranean basin. *Hy-  
686 drology and Earth System Sciences Discussions* 9, 523–533.
- 687 Yang, Y.E., Wi, S., Ray, P.A., Brown, C.M., Khalil, A.F., 2016. The future  
688 nexus of the brahmaputra river basin: Climate, water, energy and food  
689 trajectories. *Global Environmental Change* 37, 16–30.
- 690 Zaniolo, M., Fletcher, S., Mauter, M.S., 2023. Multi-scale planning model  
691 for robust urban drought response. *Environmental Research Letters* 18,  
692 054014.